

On the Reliability of Electrical Drives for Safety-Critical Applications

**G. Scelba, °G. De Donato, *G. Scarcella, °F. Giulii Capponi, *M. Cacciato, and °F. Caricchi*

**University of Catania, Italy °Sapienza – University of Rome, Italy*

Abstract

The aim of this work is to present some issues related to fault tolerant electric drives, which are able to overcome different types of faults occurring in the sensors, in the power converter and in the electrical machine, without compromising the overall functionality of the system. These features are of utmost importance in safety-critical applications. In this paper, the reliability of both commercial and innovative drive configurations, which use redundant hardware and suitable control algorithms, will be investigated for the most common types of fault: besides standard three phase motor drives, also multiphase topologies, open-end winding solutions, multi-machine configurations will be analyzed, applied to various electric motor technologies. The complexity of hardware and control strategies will also be compared in this paper, since this has a tremendous impact on the investment costs.

Reliability

The use of electrical drives as a means to achieve efficient electromechanical energy conversion is a key element in the global vision of sustainable development that is compatible with the safeguard of the environment and of the future generations. For example, in automotive applications, electrical drives are able to guarantee low emissions, high efficiency in the energy conversion process, compact size and reduced weight. Furthermore, in automotive and more in general in safety critical applications, it is also necessary to guarantee high levels of reliability.

Reliability can be defined as the attitude of the drive or of one of its parts to perform its intended function for a specified time interval, under specific operating conditions. Conversely, the lifetime T_{part} of the part is the amount of time during which it performs its intended function. By nature, T_{part} is a continuous random variable with a probability density function $f_{part}(t)$, known as the time to failure distribution, [1]. The probability that a part will survive beyond a specified time t , $P(T_{part} > t)$, is its reliability function, $R_{part}(t)$. This is formally defined in probability theory as a complementary cumulative distribution function:

$$R_{part}(t) = P(T_{part} > t) = \int_t^{+\infty} f_{part}(x) dx \quad (1)$$

Assuming the part to be non-repairable, the mean time to failure (MTTF) of a single part, $MTTF_{part}$, is defined as the mean value of T_{part} :

$$MTTF_{part} = \int_0^{+\infty} t f_{part}(t) dt = \int_0^{+\infty} R_{part}(t) dt \quad (2)$$

Moreover, the failure rate of the part, $h_{part}(t)$, is defined as the conditional probability that a fault may occur in a time interval dt , given that the part has not failed before time t . It is formally defined as:

$$h_{part}(t) = \frac{f_{part}(t)}{R_{part}(t)} = -\frac{d[\log(R_{part}(x))]}{dx} \quad (3)$$

Based on this, it is also possible to express $R_{part}(t)$ as:

$$R_{part}(t) = e^{\left(-\int_0^t h_{part}(x) dx\right)} \quad (4)$$

Figure 1 shows a typical life cycle curve for which the failure rate is plotted as function of time; many components fail very soon after they are put into service. Failures within this period are caused by defects and poor design that cause a component to be retained damaged. These are called infant mortality failures and the failure rate in this period is relatively high. After a component reaches a certain age, it enters the period where it begins to wear out, and failures start to increase. The period where failures start to increase is called the wear out phase of component life. When faults due to infant mortality and to ageing are not taken into account, it is quite common to assign a constant failure rate to many electronic components: $h_{part}(t) = \lambda$. Thus, the reliability function of a single component of the drive becomes an exponential distribution:

$$R_{part}(t) = e^{-(\lambda t)} \quad (5)$$

For this distribution, it can easily be calculated that:

$$MTTF_{part} = \frac{1}{\lambda} \quad (6)$$

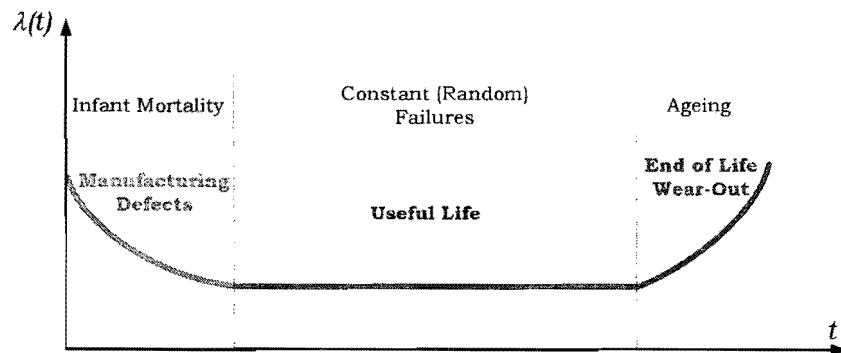


Figure 1 Bathtub curve of Failure Rate $\lambda(t)$

Reliability in Electrical Drives

The above definitions can be applied to each component of an electrical drive, leading to the results shown in Tab.I. It can be noted that the highest failure rates are associated with the position sensor, with the bearings and with the winding of the electrical machine, strongly affecting the useful life of the drive. This is one of the reasons to try to remove these components from the electrical drive system through solutions technically named as sensorless drives and bearingless drives, for instance, [2]-[7].

Table I: Failure Rates and MTTF of some electrical drive components.

Components	Failure Rate λ (h^{-1})	Failure in Time FIT (10^9h)	MTTF (h)
Encoder	11.2×10^{-7}	1120	892857
Current Sensors	2×10^{-7}	200	5000000
IGBT+Gate Drive	2×10^{-7}	200	5000000
Capacitors	2.5×10^{-7}	250	4000000
Windings	3.2×10^{-6}	320	277778
Bearings	6.4×10^{-6}	640	156250

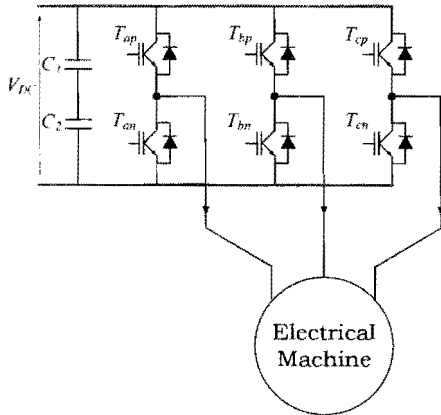
Combining the failure rates of the single components, it is possible to determine the failure rate of a drive; for example, it is well known that in a standard three-phase inverter, Fig. 2, the failure of one component compromises the functionality of the entire drive. From a reliability-engineering point of view, this is a series reliability architecture, in which the reliability of the system is equal to the product of the reliability of the single components:

$$R_s(t) = R_1(t) \cdot R_1(t) \cdot K \cdot R_n(t) = \prod_{i=1}^n R_i(t) \quad (1)$$

If we assume that the reliability functions are of the type indicated in (5), equation (7) then can be expressed as a simple relationship between MTTF and λ :

$$R_i(t) = e^{-(\lambda_i t)} \Rightarrow \lambda_s = \sum_{i=1}^n \lambda_i \quad R_s(t) = e^{-(\lambda_s t)} \Rightarrow MTTF_s = \frac{1}{\lambda_s} = \frac{1}{\sum_{i=1}^n \lambda_i} \quad (2)$$

From (8) it can be seen that the reliability of the inverter is less than the reliability of the weakest among its components. A practical example of the calculation of the failure rate and MTTF for the three-phase inverter shown in Fig.2 is reported in (9) and (10), considering the failure rates of Table I.



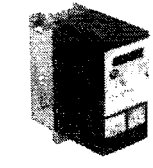

$$\lambda_s = \sum_{i=1}^6 \lambda_{i_IGBT} + \sum_{i=1}^2 \lambda_{i_Cap} = 6 \times 200 + 2 \times 250 = 1700 FIT \quad (9)$$

$$MTTF_s = \frac{1}{\lambda_s} 10^9 = 588235 h \quad (10)$$

Figure 2 Standard Three-Phase Inverter Topology.

Tab.II shows the MTTF reported in the datasheets of two commercial electrical drives and the respective reliabilities after one and five years of 24h operation. It can be seen that the probability of failure in both time intervals is still quite low, although it progressively increases with time. The MTTF is less than the one calculated in (10) because, for a commercial product, it is necessary to take into account additional components, such as the control unit, the current and position sensors and the rectifier.

Table II: MTTFs of commercial variable speed drives.

	<p>Schneider: ATV312H018M2 variable speed drive 0.18kW- 200..240 V</p>	<p>MTTF 400000h $R_s(8760) = e^{-\left(\frac{8760}{400000}\right)} \cong 98\%$</p>
	<p>Yaskawa: SIGMA II SGD7-30DE-S2 AMP 400V 3PH 3KW</p>	<p>$R_s(5 \cdot 8760) = e^{-\left(\frac{5 \cdot 8760}{400000}\right)} \cong 89.6\%$</p>

Fault Tolerant Electrical Drives

Although electrical drives have high values of MTTF and thus of reliability, in some cases, such as in aerospace or automotive applications, it is imperative to ensure the safety of human beings, machines and environment, while guaranteeing maximum efficiency and flexibility. These results are obtained by further increasing the reliability of the drives, making them able to guarantee correct operations even in the event of faults. This category of electrical drives is known as "fault tolerant". Many topologies of fault tolerant drives exist and have different abilities in mitigating the effects of specific faults; nonetheless, the general characteristics of a fault tolerant drive are:

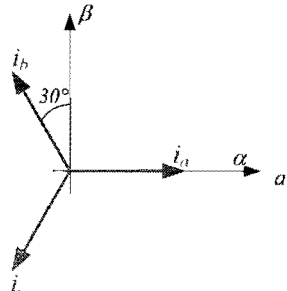
- the detection and identification of faults;
- the isolation of faults;
- the reconfiguration of the drive, either by using reserve components or by redistributing the process to working components;
- the restoration of a fault-free operating condition

Drives tolerant to Current Sensor Failures

Some of the many ways to make a drive tolerant to current sensor faults are described in [8]-[15]. A simple technique is the one described in [8], where three fault indicators are obtained, C_{ri} , $i=1,2,3$, starting from the stator three phase currents, transformed in an orthogonal stationary reference frame $\alpha\beta$, (11), (12). These three fault indicators give the projections of the rotating stator current vector on the $\alpha\beta$ axes, by using different combinations of the measured currents and using the condition $i_a+i_b+i_c=0$ which is valid during normal operation of the drive. In this condition, the three indicators coincide at each instant with the amplitude of the reference current I_{ref} .

$$\begin{cases} i_{\alpha 1} = i_a \\ i_{\alpha 2} = -(i_b + i_c) \end{cases} \quad (11)$$

$$\begin{cases} i_{\beta 1} = \frac{1}{\sqrt{3}}(i_b - i_c) \\ i_{\beta 2} = \frac{1}{\sqrt{3}}(i_a + 2i_b) \\ i_{\beta 3} = -\frac{1}{\sqrt{3}}(i_a + 2i_c) \end{cases} \quad (12)$$

$$\begin{cases} C_{r1} = i_{\alpha 2}^2 + i_{\beta 1}^2 \\ C_{r2} = i_{\alpha 1}^2 + i_{\beta 3}^2 \\ C_{r3} = i_{\alpha 1}^2 + i_{\beta 2}^2 \end{cases}$$


The fault is detected simply by monitoring the condition $ia+ib+ic=0$; when the sum of the three currents exceeds a specified threshold ϵ , a flag G which indicates a fault changes state. The identification of a faulty sensor is obtained by comparing each fault indicator C_{ri} with I_{ref} . The C_{ri} that has been obtained with healthy sensors shows no difference with respect to normal operating conditions. The remaining two indicators will have amplitudes that exceed that of I_{ref} , beyond a threshold ϵ , and active flags F_i . A unique combination for each faulty sensor is obtained, as shown in table III. After having detected the fault and identified the broken sensor, it is necessary to reconfigure the system to guarantee continuity of service. A simple solution consists in combining the current projections on the $\alpha\beta$ reference frame so as to select the two current measurements that don't include the faulty sensor measurement.

$$\begin{aligned} i_\alpha &= K_1 i_{\alpha_2} + K_2 i_{\alpha_1} + K_3 i_{\alpha 1} + K_4 i_{\alpha_1} \\ i_\beta &= K_1 i_{\beta_1} + K_2 i_{\beta_3} + K_3 i_{\beta 2} + K_4 i_{\beta_2} \end{aligned} \quad (13)$$

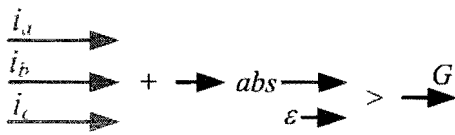


Figure 3 Fault detection

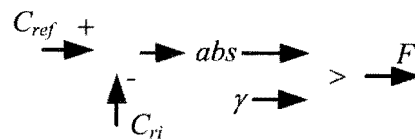


Figure 4 Broken sensor identification

Table III:

Faulty Sensor	G	F ₁	F ₂	F ₃	K ₁	K ₂	K ₃	K ₄
Phase a	1	0	1	1	1	0	0	0
Phase b	1	1	0	1	0	1	0	0
Phase c	1	1	1	0	0	0	1	0
No Fault	0	0/1	0/1	0/1	0	0	0	1

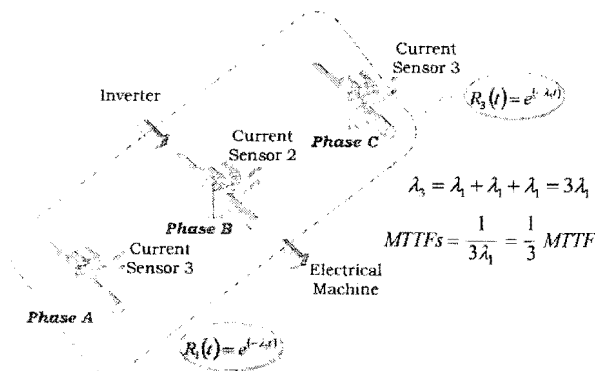


Figure 5 Structure of the current sensing system.

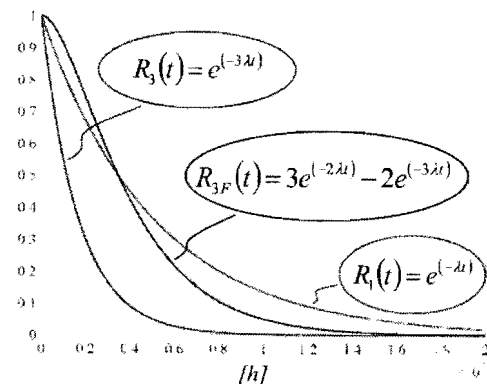


Figure 6 Comparison between the reliability of a single sensor R_1 , of the traditional sensing system R_3 and of the fault tolerant system R_{3F} .

The above described fault tolerant solution allows a significant increase in the reliability of the current sensing system, as visible in (14), obtained by applying the functional rules for "k-out-of-n" Systems, [1]; the MTTF of the above described method $MTTF_{3F}$ has been compared with that of the standard acquisition current sensing system $MTTF_{3F}$, obtaining a more than double increase in the current sensing system reliability.

$$MTTF_{3F} = \frac{5}{6} MTTF_1, \quad MTTF_3 = \frac{1}{3} MTTF_1, \quad \frac{MTTF_{3F}}{MTTF_3} = \frac{15}{6} = 2.5$$

(14)

Drives Tolerant to Position Sensors Faults

Recently, it has been shown that position-sensing systems based on discrete low-resolution sensors, such as binary Hall-effect sensors, may become fault-tolerant, [16], [17].

A well-known layout uses three sensors, H_1, H_2, H_3 , displaced 120 electrical degrees apart. Each sensor has a binary output equal to 0 or 1 depending on the rotor flux position. This layout provides a 60 electrical degree resolution, i.e. 3 bits per pole pair. Fig.7 shows the locus of the $H_{\alpha\beta}$ vector, obtained by applying the following transformations to the Hall-effect sensor signals:

$$\begin{pmatrix} H_a \\ H_b \\ H_c \end{pmatrix} = 2 \begin{pmatrix} H_1 \\ H_2 \\ H_3 \end{pmatrix} - 1$$

(15)

$$\begin{pmatrix} H_\alpha \\ H_\beta \end{pmatrix} = \frac{\pi}{4} \begin{bmatrix} 1 & -\frac{1}{2} & -\frac{1}{2} \\ 0 & \frac{\sqrt{3}}{2} & -\frac{\sqrt{3}}{2} \end{bmatrix} \begin{pmatrix} H_a \\ H_b \\ H_c \end{pmatrix}$$

(16)

As the rotor revolves, $H_{\alpha\beta}$ moves in a quantized fashion jumping from one direction to the next, every 60° electrical, forming the hexagonal locus shown in Fig.7. When one of the Hall-effect sensors fails, its output goes to logical 0 or 1 indefinitely. A total of six different single faults are possible. For example, Fig.8 shows the $H_{\alpha\beta}$ locus in the event of a $H_1=1$ fault: the locus becomes rhomboidal, splitting the reference frame into four sectors. Two sectors are 60° wide, while the other two are 120° wide. A zero vector, $H_{\alpha\beta 7}$, appears when the sensors' states are (111); this is not present during normal operation.

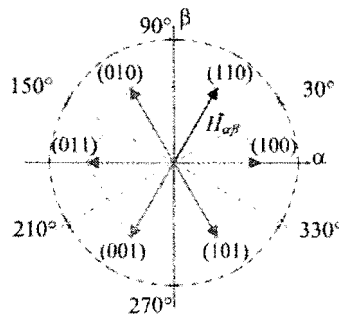


Figure 7 Quantized rotating position vector $H_{\alpha\beta}$ loci for a 3 BPP low-resolution position-sensing system, [16].

A similar zero vector is also present for faults in which one sensor output goes to 0, i.e. for a (000) combination. The shapes of the $H_{\alpha\beta}$ loci are the same for all six single faults. However, the position of the loci within the reference frame is unique for each fault. If a fault detection, identification and compensation algorithm is not used, a failure of any one of the three Hall-effect sensors will compromise the entire sensing system. In this case, the reliability function of the sensing system, $R_{3\Sigma Hall}(t)$, is equal to the product of the reliability functions of each sensor:

$$R_{3\Sigma Hall}(t) = R_{Hall,1}(t) \cdot R_{Hall,2}(t) \cdot R_{Hall,3}(t) = R_{Hall}^3(t) \quad (17)$$

and the MTTF for such an arrangement is:

$$MTTF_{3\Sigma Hall} = \frac{1}{\sum_{k=1}^3 \lambda_k} = \frac{1}{3\lambda_{Hall}} = \frac{1}{3} MTTF_{Hall} \quad (18)$$

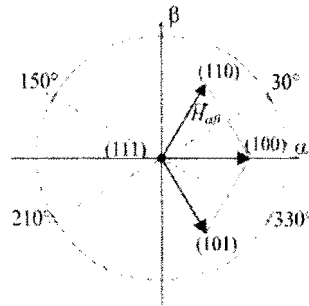


Figure 8 Quantized locus $H_{\alpha\beta}$ in the stationary reference frame for a $H_i = 1$ single fault. [16].

A sensor fault can be detected when a zero vector appears in the $H_{\alpha\beta}$ locus. Since the locus associated to each fault is unique, the broken sensor and fault type are identified unambiguously by the phase of $H_{\alpha\beta}$ in the sector following the zero vector. Following fault detection and identification, the fault can always be compensated by appropriately modifying the position and speed algorithm that is implemented in the motor control system, [16]. By providing the appropriate fault compensation, the sensing system possesses a triple modular redundancy and constitutes a parallel reliability architecture. In this case, it can be shown that the reliability function, $R_{3//Hall}(t)$, is equal to:

$$R_{3//Hall}(t) = 1 - [1 - R_{Hall}]^3 \quad (19)$$

This implies that the reliability of the system will be larger than that of each sensor. It can be calculated that the MTTF for such an arrangement is equal to:

$$MTTF_{3//Hall} = \frac{1}{\lambda_{Hall}} \sum_{k=1}^3 \left(\frac{1}{k} \right) = \frac{11}{6\lambda_{Hall}} = \frac{11}{6} MTTF_{Hall} \quad (20)$$

By comparing (8) and (10), it can be seen that the MTTF improves by a factor of 5.5 when a fault detection, identification and compensation algorithm is used. According to the limited literature available, estimates of Hall-effect sensor MTTFs are in the range of 10^6 - 10^8 hours, with the former value suggested for use in extreme environmental conditions. For example, for an $MTTF_{Hall} = 1.8 \cdot 10^7$ hours, $MTTF_{3\Delta Hall} = 6 \cdot 10^6$ hours and $MTTF_{3//Hall} = 3.3 \cdot 10^7$ hours.

Fault Tolerant Drive Topologies

In order to mitigate the effect of faults that arise in the switches, the traditional structure of the inverter may be modified by adding circuit elements that are required to identify and isolate the fault [18]-[45]. Immediately after a fault, the converter is reconfigured so as to restore, partially or fully, the performances of the drive. A low cost solution which allows to survive a fault is shown in Fig.9, [27], [28]. This topology includes six ultra-rapid fuses, three triacs and an additional leg. When one of the switches fails due to a short circuit or an open circuit, the related fuse opens the leg and activates the triac connected between the faulty leg and the additional leg. The additional leg is commanded with the same switching commands sent to the gate drives of the damaged leg. In this way, normal operation is restored and the same modulation strategy and control structure is maintained. Unfortunately, this fault tolerant topology cannot handle an open phase.

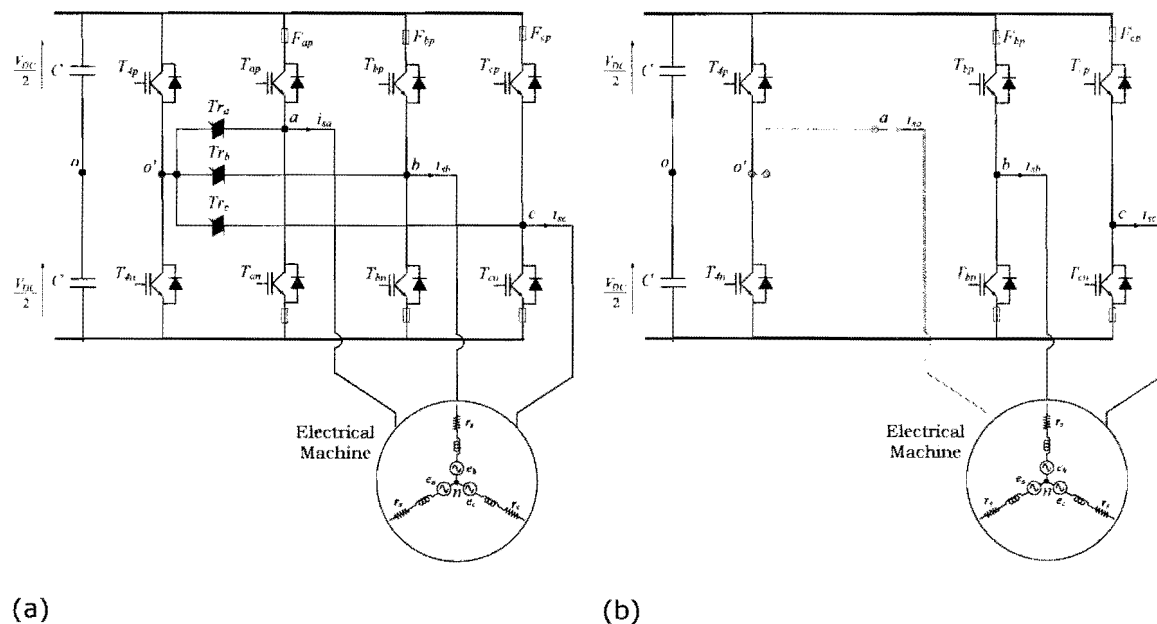


Figure 9 Fault Tolerant Three Phase Inverter Topology (1).

In order to mitigate the effect of an open phase fault, the topology shown in Fig.10 can be used, [27], [28]. Such a fault can be handled by exploiting the connection between the center of the star of the stator winding and the mid-point of the additional leg. In this case, after the onset of the fault, the same rotating magnetic field is obtained in the airgap by modifying the currents that flow in the two healthy phases, as indicated in (21).

$$\begin{cases} i_i(t) = \sqrt{3}I \cos(\omega_e t + \phi + \gamma_1) \\ i_j(t) = \sqrt{3}I \cos(\omega_e t + \phi + \gamma_2) \end{cases} \quad (i, j) = \begin{cases} \left(-\frac{5}{6}\pi, \frac{5}{6}\pi\right) \text{ open phase 'a'} \\ \left(\frac{\pi}{6}, \frac{\pi}{2}\right) \text{ open phase 'b'} \\ \left(-\frac{\pi}{6}, -\frac{\pi}{2}\right) \text{ open phase 'c'} \end{cases} \quad (21)$$

From an operational point of view, the control structure may remain similar to that of a healthy drive, as shown in the example reported in Fig.11. The current vector control loop is modified in the reference frame transformations with new matrices **A**, **B**, **R_r** and **R_v**, in which the terms depend on the faulty phase, [19],[20].

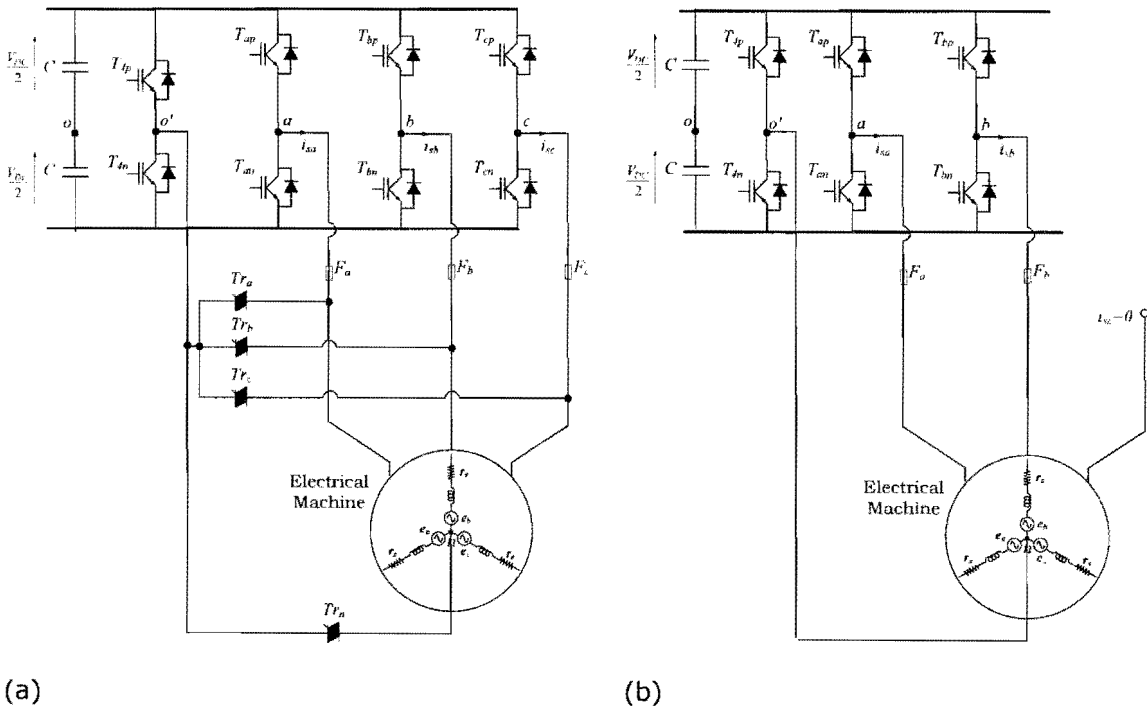


Figure 10 Fault Tolerant Topology (2).

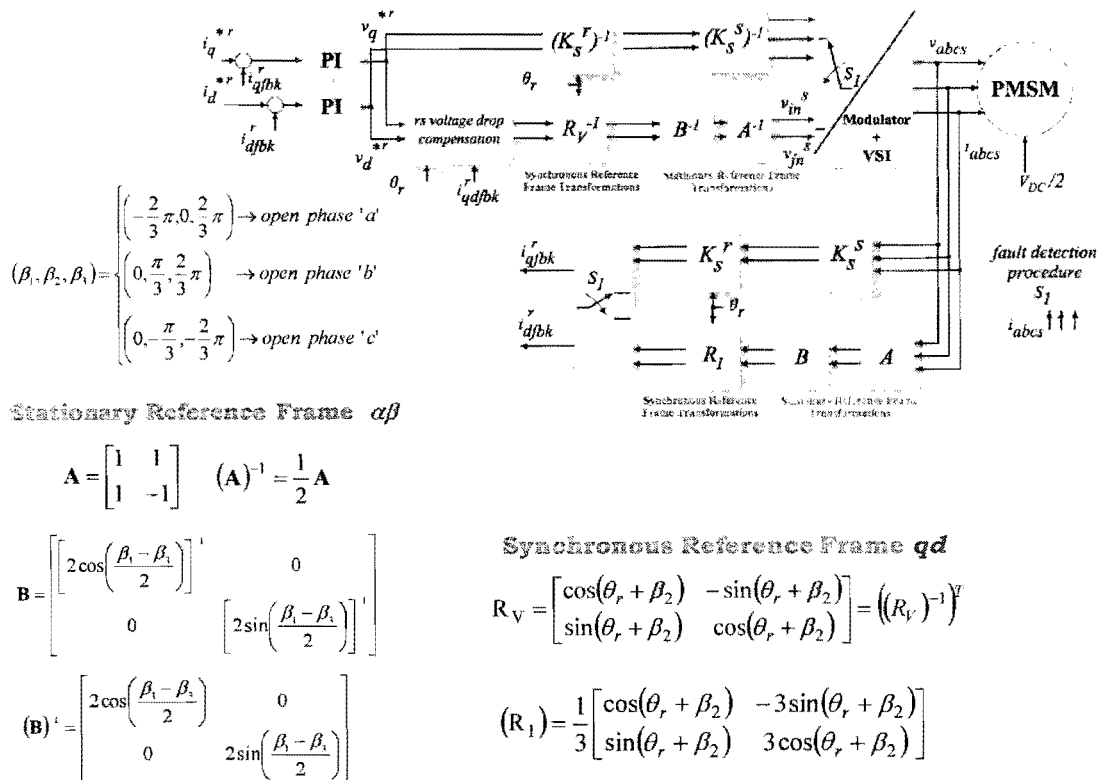


Figure 11 Fault Tolerant Current Vector Control Strategy.

Fault Tolerant Multi-Phase Motor Drives

In order to increase the ability to operate in the presence of multiple faults, some topologies have been developed which include electrical machines with a number of phases greater than three, as shown in Fig.12, [31]-[45]. In this way, the drive is able to manage more than one fault and maintain satisfactory dynamic and energetic performances (i.e. limited torque ripple and limited increase of losses); on the other hand, specific control logic is required in the selection of the current references.

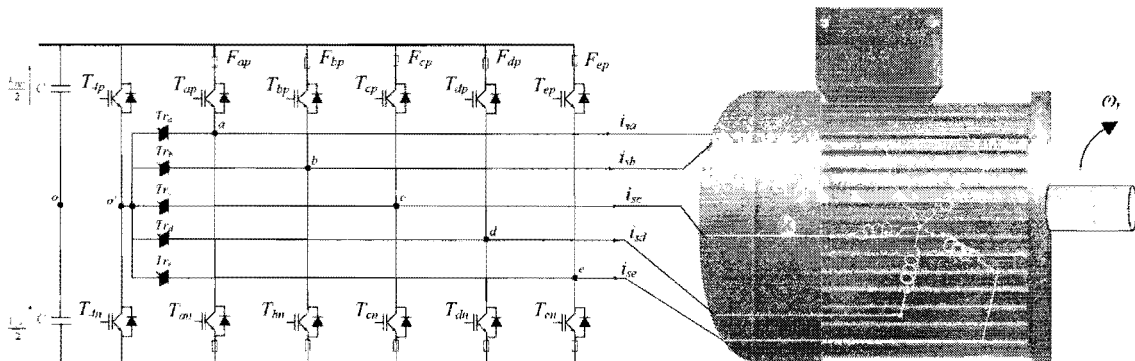


Figure 12 Fault Tolerant Multi-Phase Motor Drive Topology

Fault Tolerant Multi-Motor Drives

In the case of multi-motor drives, the reliability of the system is increased by allowing the single constituent modules to operate in parallel or sequentially, [1], [15]. If one of the modules is damaged it is de-energized and the remaining modules operate and guarantee service even for long periods of operation. This modular configuration is tolerant to various types of machine faults (inter-turn, phase to phase and phase to ground short circuits) and of sensor faults (current and voltage sensors). On the other hand, this flexibility entails an increase in costs and in the complexity of the system.

In the case of active redundancy, the modules are operated permanently in parallel and each drive is capable of controlling the torque and speed profiles that are required by the application. The continuity of operation of the system is ensured as long as a single drive is operating correctly; moreover, it is demonstrated that the MTTF is increased by 50% with respect to the case of a single drive.

$$MTTF_{Redundancy(1)} = \frac{3}{2} \frac{1}{\lambda_{Module}} = \frac{3}{2} MTTF_{Module} \quad (22)$$

If the same topology is managed by using a passive or sequential redundancy strategy, module 2 becomes operational only if module 1 undergoes a fault. Specifically, when module 1 is faulty, an ideal commutation system having negligible failure rate and operating instantaneously will de-activate module 1 and activate module 2. This functional configuration in which the two modules operate in parallel and sequentially guarantees that the MTTF is doubled (23).

$$MTTF_{Redundancy(2)} = \frac{2}{\lambda_{Module}} = 2 MTTF_{Module} \quad (23)$$

This last solution requires periodic inspections of the stand-by module; furthermore, the overall reliability is strongly dependent on that of the commutation system and the commutation transient might compromise the continuity of service.

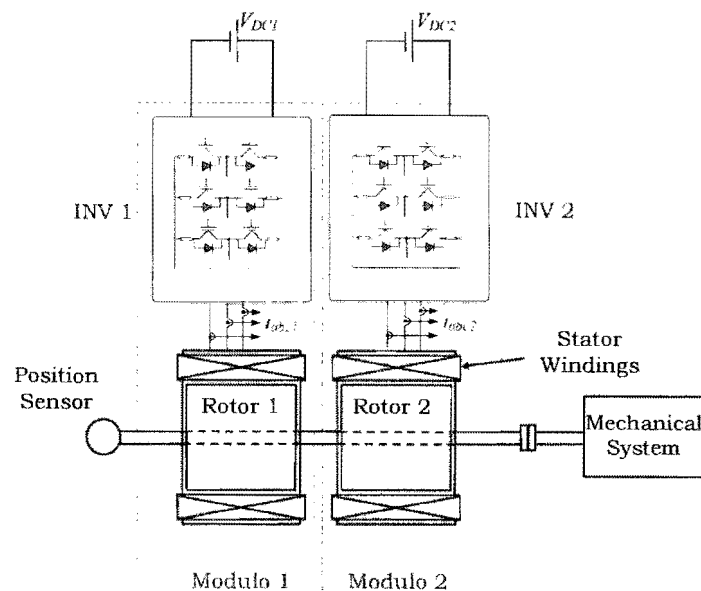


Figure 13 Modular configuration of Fault Tolerant Drives

Increase in Reliability via Sensorless Control Strategies

In order to further increase the reliability of the system it is possible to implement control techniques in which the position sensor is eliminated replaced by machine self-sensing

[2]-[7]. These technical solutions, known as sensorless controls reduce the complexity of the drive, increase the reliability of the system and reduce the maintenance and wiring; they are able to guarantee performances that are similar to "sensored" control in terms of accuracy and dynamics. Furthermore, they must be able to guarantee the continuity of service in the even of faults, if they are integrated into sensorless-fault tolerant drives. Sensorless controls use a fundamental excitation machine model in the medium to high speed range, while they use high frequency signal injection at zero and low speeds.

Model based sensorless techniques use estimation algorithms or observers to obtain an estimate of the rotor flux position and of the speed of rotation. Signal injection based techniques instead are useful only if the machine has a structural or magnetic saliency which is detectable by injecting additional high frequency fields.

Conclusions

This paper has given a brief overview of how reliability analysis can be applied to electrical drives, operating in safety-critical applications. It has been shown how standard drives may be inadequate and how using hardware or software modifications or a combination of both may increase the reliability considerably. Some state of the art solutions have been described, indicating the pros and cons.

References

- [1]. Patrick D. T. O'Connor, Andre Kleyner, *Practical Reliability Engineering*, Fifth Edition, A John Wiley & Sons, Ltd., Publication, 2012.
- [2]. A. Consoli, G. Scarcella, G. Scelba, A. Testa, D. A. Triolo, *Sensorless Rotor Position Estimation in Synchronous Reluctance Motors Exploiting a Flux Deviation Approach*, IEEE Transaction on Industry Applications, September/October 2007, vol. 43, no. 5, pp. 1266-1273.
- [3]. Y.D. Yoon, S.-K. Sul, S. Morimoto and K. Ide, *High-Bandwidth Sensorless Algorithm for AC Machines Based on Square-Wave-Type Voltage Injection*, IEEE Transactions on Industry Applications, May/June 2011, vol.47, no.3, pp. 1361-1370.
- [4]. S. Sato, H. Iura, K. Ide, S.-K. Sul, *Three years of industrial experience with sensorless IPMSM drive based on high frequency injection method*, 2011 Symposium on Sensorless Control for Electrical Drives (SLED 2011), pp. 74-79.
- [5]. S.-C. Yang, R. D. Lorenz, *Comparison of Resistance-Based and Inductance-Based Self-Sensing Controls for Surface Permanent- Magnet Machines Using High-Frequency Signal Injection*, IEEE Transactions on Industry Applications, May/June 2012, vol. 48, no. 3, pp. 977-986.
- [6]. J. Holtz, *Sensorless control of induction motor drives*, Proceedings of the IEEE, August 2002, vol. 90, n. 8, pp. 1359-1394.
- [7]. S. Alireza Davari, Davood Arab Khaburi, Fengxiang Wang, Ralph M. Kennel, *Using Full Order and Reduced Order Observers for Robust Sensorless Predictive Torque Control of Induction Motors*, July 2012, IEEE Transactions on Power Electronics, vol. 27, n. 7, pp. 3424-3433.
- [8]. Imen Bahri, Ilhem Slama-Belkhdja, Eric Monmasson, *FPGA-based real-time simulation of fault tolerant current controllers for power electronics*, 2009 IEEE International Symposium on Industrial Electronics, pp. 378-383.
- [9]. Ali Mohamad Bazzi, *designing better induction motor drive systems from efficiency, reliability, and power electronics perspectives*, PhD Thesis, University of Illinois (USA), 2010.
- [10]. Chia-Chou Yeh, *fault tolerant operations of induction motor-drive systems*, PhD Thesis, Marquette University (USA), 2008.
- [11]. A. Gaeta *Fault Tolerant Sensorless Permanent Magnet Synchronous Motor Drives*, PhD Thesis, University of Catania, Italy, 2011.
- [12]. Michele Dai Prè, *Analysis and design of Fault-Tolerant drives*, PhD Thesis, University of Padova, Italy, 2008.
- [13]. Jingwei Zhu, Modelling, *Simulation and Implementation of a Fault Tolerant Permanent Magnet AC Motor Drive with Redundancy*, PhD Thesis, University of Adelaide, 2008.
- [14]. James Alexander Haylock, *Fault Tolerant Drives for Safety Critical Applications*, PhD Thesis, University of Newcastle upon Tyne, 1998.
- [15]. Rammohan Rao Errabelli, *Inverter and Controller for Highly Available Permanent Magnet Synchronous Drives*, PhD Thesis, University of Darmstadt, 2012.
- [16]. Giacomo Scelba, Giulio De Donato, Giuseppe Scarcella, Fabio Giulii Capponi, Filippo Bonaccorso, *Fault-Tolerant Rotor Position and Velocity Estimation Using Binary Hall-Effect Sensors for Low-Cost Vector Control Drives*, IEEE Transactions on Industry Applications, vol. 50, n.5, September/October 2014, pp. 3403-3413.

- [17]. Giacomo Scelba, Giulio De Donato, Mario Pulvirenti, Fabio Giulii Capponi, Giuseppe Scarcella, *Hall-Effect Sensor Fault Detection, Identification, and Compensation in Brushless DC Drives*, IEEE Transactions on Industry Applications, March/April 2016, vol. 52, n.2, pp. 1542-1554.
- [18]. Juan Colmenares, Diane-Perle Sadik, Patrik Hilber, Hans-Peter Nee, *Reliability Analysis of a High-Efficiency SiC Three-Phase Inverter*, IEEE Journal of Emerging and Selected Topics in Power Electronics, vol. 4, n.3, September 2016, pp. 996-1006.
- [19]. Alberto Gaeta, Giacomo Scelba, Alfio Consoli, *Modeling and Control of Three-Phase PMSMs Under Open-Phase Fault*, IEEE Transactions on Industry Applications, January/February 2013, vol. 49, n.1, pp. 74-83.
- [20]. Mario Pulvirenti, Giuseppe Scarcella, Giacomo Scelba, Mario Cacciato, Antonio Testa, *Fault-Tolerant AC Multidrive System*, IEEE Journal of Emerging and Selected Topics in Power Electronics, June 2014, vol. 2, n.2, pp.224-235.
- [21]. K. Rothenhagen, F. W. Fuchs, *Performance of diagnosis methods for IGBT open circuit faults in three phase voltage source inverters for AC variable speed drives*, 2005 European Conference on Power Electronics and Applications, 2005, pp. 1-10.
- [22]. R. Peugeot, S. Courtine, J. -P. Rognon, *Fault detection and isolation on a PWM inverter by knowledge-based model*, IEEE Transactions on Industry Applications, November/December 1998, vol. 34, n.6, pp. 1318-1326.
- [23]. Jorge O. Estima, Nuno M. A. Freire, A. J. Marques Cardoso, *Recent advances in fault diagnosis by Park's vector approach*, 2013 IEEE Workshop on Electrical Machines Design, Control and Diagnosis (WEMDCD), pp. 279-288.
- [24]. Behrooz Mirafzal, *Survey of Fault-Tolerance Techniques for Three-Phase Voltage Source Inverters*, IEEE Transactions on Industrial Electronics, October 2014, vol. 61, n. 10, pp. 5192-5202.
- [25]. R. R. Schoen, T. G. Habetler, F. Kamran, R. G. Bartfield, *Motor bearing damage detection using stator current monitoring*, IEEE Transactions on Industry Applications, November/December 1995, vol. 31, n. 6, pp. 1274-1279.
- [26]. Ke Ma, Huai Wang, Frede Blaabjerg, *New Approaches to Reliability Assessment: Using physics-of-failure for prediction and design in power electronics systems*, IEEE Power Electronics Magazine, December 2016, vol. 3, n. 4, pp. 28-41.
- [27]. B. A. Welchko, T. A. Lipo, T. M. Jahns, S. E. Schulz, *Fault tolerant three-phase AC motor drive topologies: a comparison of features, cost, and limitations*, IEEE Transactions on Power Electronics, July 2004, vol. 19, n.4, pp. 1108-1116.
- [28]. R. L. de Araujo Ribeiro, C. B. Jacobina, E. R. C. da Silva, A. M. N. Lima, *Fault-tolerant voltage-fed PWM inverter AC motor drive systems*, IEEE Transactions on Industrial Electronics, April 2004, vol. 51, n. 2, pp. 439-446.
- [29]. Andr M. S. Mendes, A. J. Marques Cardoso, *Fault-Tolerant Operating Strategies Applied to Three-Phase Induction-Motor Drives*, IEEE Transactions on Industrial Electronics, December 2006, vol. 53, n. 6, pp. 1807-1817.
- [30]. Oskar Wallmark, Lennart Harnefors, Ola Carlson, *Control Algorithms for a Fault-Tolerant PMSM Drive*, IEEE Transactions on Industrial Electronics, August 2007, vol. 54, n. 4, pp. 1973-1980.
- [31]. Ahmed Sayed-Ahmed, Nabeel A. O. Demerdash, *Fault-Tolerant Operation of Delta-Connected Scalar- and Vector-Controlled AC Motor Drives*, IEEE Transactions on Power Electronics, June 2011, vol. 27, n. 6, pp. 3041-3049.

- [32]. Behrooz Mirafzal, *Survey of Fault-Tolerance Techniques for Three-Phase Voltage Source Inverters*, IEEE Transactions on Industrial Electronics, October 2014, vol. 61, n. 10, pp. 5192-5202.
- [33]. Nicola Bianchi, Silverio Bolognani, Michele Dai Pre, *Strategies for the Fault-Tolerant Current Control of a Five-Phase Permanent-Magnet Motor*, IEEE Transactions on Industry Applications, July/August 2007, vol. 43, n. 4, pp. 960-970.
- [34]. Suman Dwari, Leila Parsa, *An Optimal Control Technique for Multiphase PM Machines Under Open-Circuit Faults*, IEEE Transactions on Industrial Electronics, May 2008, vol. 55, n. 5, pp. 1988-1995.
- [35]. Malakondaiah Naidu, Suresh Gopalakrishnan, Thomas W. Nehl, *Fault-Tolerant Permanent Magnet Motor Drive Topologies for Automotive X-By-Wire Systems*, IEEE Transactions on Industry Applications, March/April 2010, vol. 46, n. 2, pp. 841-848.
- [36]. Angelo Tani, Michele Mengoni, Luca Zarri, Giovanni Serra, Domenico Casadei, *Control of Multiphase Induction Motors With an Odd Number of Phases Under Open-Circuit Phase Faults*, IEEE Transactions on Power Electronics, February 2012, vol. 27, n. 2, pp. 565-577.
- [37]. Luigi Alberti, Nicola Bianchi, *Experimental Tests of Dual Three-Phase Induction Motor Under Faulty Operating Condition*, IEEE Transactions on Industrial Electronics, May 2012, vol. 59, n. 5, pp. 2041-2048.
- [38]. John W. Bennett, Glynn J. Atkinson, Barrie C. Mecrow, David J. Atkinson, *Fault-Tolerant Design Considerations and Control Strategies for Aerospace Drives*, IEEE Transactions on Industrial Electronics, May 2012, vol. 59, n. 5, pp. 2049-2058.
- [39]. Ali Mohammadpour, Siavash Sadeghi, Leila Parsa, *A Generalized Fault-Tolerant Control Strategy for Five-Phase PM Motor Drives Considering Star, Pentagon, and Pentacle Connections of Stator Windings*, IEEE Transactions on Industrial Electronics, January 2014, vol. 61, n. 1, pp. 63-75.
- [40]. Rammohan Rao Errabelli, Peter Mutschler, *Fault-Tolerant Voltage Source Inverter for Permanent Magnet Drives*, IEEE Transactions on Power Electronics, February 2012, vol. 27, n. 2, pp. 500-508.
- [41]. Yantao Song, Bingsen Wang, *Analysis and Experimental Verification of a Fault-Tolerant HEV Powertrain*, IEEE Transactions on Power Electronics, December 2013, vol. 28, n.12, pp. 5854-5864.
- [42]. Chee-Shen Lim, Emil Levi, Martin Jones, Nasrudin Abd Rahim, Wooi-Ping Hew, *A Fault-Tolerant Two-Motor Drive With FCS-MP-Based Flux and Torque Control*, IEEE Transactions on Industrial Electronics, December 2014, vol. 61, n.12, pp. 6603-6614.
- [43]. Ayman M. EL-Refaie, Manoj R. Shah, Kum-Kang Huh, *High-Power-Density Fault-Tolerant PM Generator for Safety-Critical Applications*, IEEE Transactions on Industry Applications, May/June 2014, vol. 50, n.3, pp. 1717-1728.
- [44]. Guillermo R. Catuogno, Guillermo O. Garcia, Roberto Leidhold, *Fault-Tolerant Inverter for Power Flow Control in Variable-Speed Four-Wire Permanent-Magnet Generators*, IEEE Transactions on Industrial Electronics, November 2015, vol. 62, n. 11, pp. 6727-6736.
- [45]. Hugo Guzman, Mario J. Duran, Federico Barrero, Luca Zarri, Blas Bogado, Ignacio Gonzalez Prieto, Manuel R. Arahal, *Comparative Study of Predictive and Resonant Controllers in Fault-Tolerant Five-Phase Induction Motor Drives*, IEEE Transactions on Industrial Electronics, January 2016, vol. 63, n. 1, pp. 606-617.